Multiphysics Design of a Klystron Buncher

Alberto Leggieri[1*], Davide Passi[1], Franco Di Paolo[1], Giovanni Saggio[1]
[1]Dept. of Electronic Engineering, University of Rome "Tor Vergata", Italy
*Corresponding author: alberto.leggieri@uniroma2.it

Abstract: The Multiphysics design of a 130 GHz klystron Buncher cavity is described in this paper. In this high frequency range, dimensions are critical and expose the device to multiple physics effects, due to the power dissipations, affecting the electromagnetic performances. The proposed device is integrated with a carbon nanotube cold cathode in order to reduce thermal expansion and an opportune airflow controls the temperature. The multiphysics design is performed on COMSOL in order to ensure the desired behavior in operative conditions. Electromagnetic fields and scattering parameters have been computed when the Buncher is subjected to multiple physics factors. The appropriate geometries and materials and can be found.

Keywords: Electron Gun, Klystron, M Multiphysics Modeling,

1. Introduction

Klystron and TWTs are the most diffused devices for broad band applications [1]. For high frequencies, close and more than millimeter and sub-millimeter wave, solid-state devices present lack of performances and vacuum tube represents the solutions. Cold cathode vacuum tubes are suitable for these bands. In a millimetric Klystron, the electron beam, emitted by a hot cathode interacts with one or more resonant cavities. In the Buncher cavity, the electron beam undergoes the force a low energy alternate field that modulates the electron velocity. As the beam has crossed a certain path, the velocity modulation become a modulation of the charge density and the beam, entering another cavity, induces an oscillating field stronger than the first, then the beam is collected at the anode. This dynamic results in an amplification of the signal. Since no magnetic field is required, klystrons are good candidates for micro vacuum tube realization [2]. Recently developed technologies have hallowed for the implementation of emitter cathodes on a micron scale, using the Photolithography suitable for miniature vacuum tubes [2]. Another Useful solution is the Micro-electro-mechanical systems (MEMS) fabrication, based on deep reactive-ion etching. The proposed device can be micro-fabricated by employing such techniques over a silicon wafer [3]. Interesting Klystron design techniques have been recently developed, allowing for the mechanical micromachining of 100 GHz Klystrons and photolithographic fabrication in the THz range [4-5]. The electron beam produced by the Electron Gun (e-Gun) needs to have very small dimensions [6]. Cold cathode technology can be useful, in order to reduce thermal expansion of the material typical of the classical thermionic cathodes.

This study shows the behavior of the Buncher while it experience the heating effects of its power dissipations, due to the wall current, and the electron gun dissipation. This analysis is based on a Multiphysics modeling. In order to control the temperature and thermal expansion, an opportune airflow is employed, cooling the system external walls. The Buncher has the shape of a reentrant cavity: Typically if the cavity radius is increased, the resonance frequency decreases, if the cavity gap increases the frequency increase. An isotropic thermal expansion may dilate the cavity Buncher mainly decreasing the operative frequency. This effect can be compensated by decreasing the surrounding temperature, requiring important cooling systems. In this paper, the use of a cooling airflow is shown by considering mechanical constraint and possible direction of thermal expansions in order to obtain the desired compensation of the frequency lowering. For this reason, in this study, an opportune airflow has been chosen to be oriented towards a certain direction for cooling off some surfaces more than others. The main model is depicted in figure 1. The solid material is a block of Silicon at which interior, the vacuum region of electron gun and Buncher is present. A layer of Silver is deposed on the internal surfaces except for the circular lateral surface of the gun that insulates the anode to the cathode.

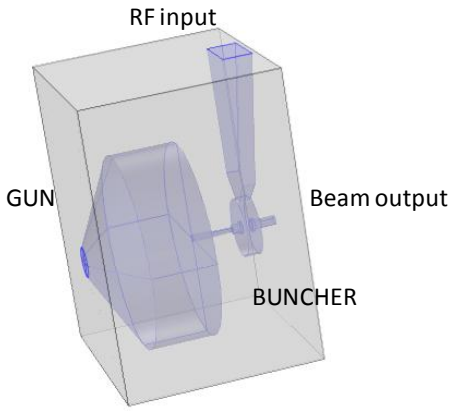

Figure 1. Electron gun connected to the Buncher

2. Use of COMSOL Multiphysics

In this study, several factors have been included as mechanical stress, thermal expansion and fluid flow, together with the electromagnetic behavior of the device, through a Finite Element Method computation based on COMSOL. In the computational model, the geometry in figure 1 has been inserted inside a box where airflow has been prescribed with other environmental conditions as temperatures and mechanical constraints. A preliminary Electromagnetic (EM) analysis is used to compute the microwave power dissipations while the Buncher receive the operative input signal (1 W mean power) at the input port.

By a Thermo-mechanical (TM) analysis, temperature and deformation have been determined considering the heating effects due to the resonator power dissipation superposed to that of the cathode (the more influent), when whose heat flux has been diffused on all the reachable components, externally cooled by an opportune airflow. For this aim, a Thermodynamic (TD) and Fluid Dynamics (FD) analysis have been coupled to a Solid Mechanics (SM) analysis obtaining temperature distribution and matrices of displacements. These displacements have been employed to produce a deformed geometry by Moving Mesh (MM) interface [7]. MM computation moved the mesh in function of the displacement found by the SM analysis. Electromagnetic calculation has been executed on the new meshes, receiving the stored temperatures. A diagram of the logical computation flow is reported in figure 2.

2.1 Electromagnetic Waves

A cylindrical cavity with rectangular reentrant cross section with sharp edges has been employed. The cavity radius has been enlarged to match a standard WR-8 waveguide long side. The resonant magnetic field, used for bunching, oscillates in a quasi TM_{010} cylindrical cavity mode. In the proposed study, a waveguide aperture is used for launching the field in cavity.

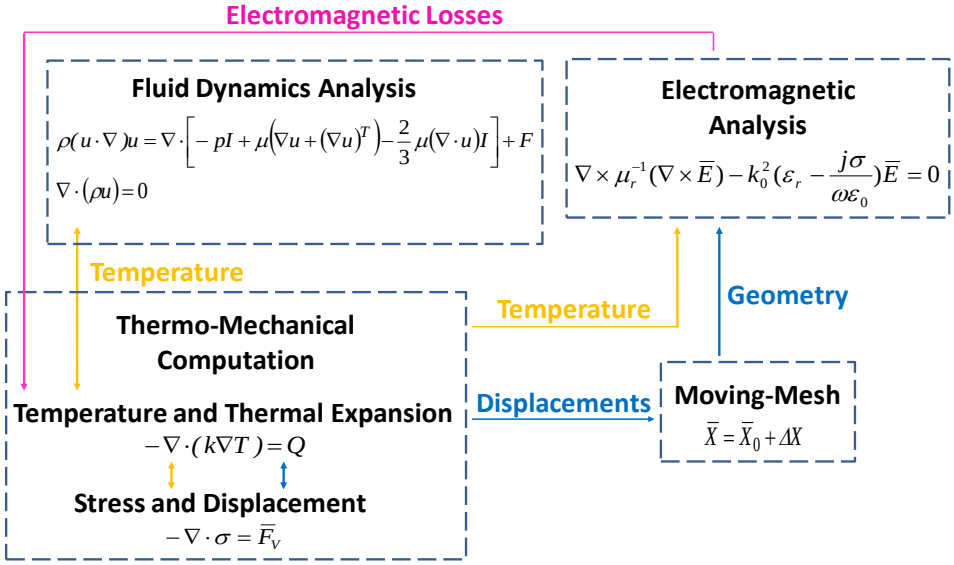

Figure 2. Computation Logical Diagram.

A doubly tapered section of two wavelengths is terminating into the cavity by a short side tapered section superposed with a double 45° shaped tapering of the long side. A tapering of the long side may lead the propagating mode under cutoff, but this solution allows for the alimentation with the correct coupling ensuring the fundamental mode over cutoff. A WR-8 waveguide flange is available at the input port for the connection of standard device.

The analytical design of the cavity has been performed solving the system of equation described by Carter [8]. By referring to this nomenclature, cavity dimensions have been set to r_1=0.16mm r_2=0.22mm r_3=0.8mm z_1=0.5mm z_2=0.16mm z_3=0.25mm. The unperturbed analytical frequency of resonance is 132.32 GHz. Basing on higher order mode operation, the cavity dimensions can be further enlarged extending the realizability to frequency operation in the THz range [4-5].

The electromagnetic analysis has been performed using the RF module of COMSOL Multiphysics to solve the wave equation in the frequency domain (1) [7].

$$\nabla \times \mu_r^{-1}(\nabla \times \bar{E}) - k_0^2(\varepsilon_r - \frac{j\sigma}{\omega\varepsilon_0})\bar{E} = 0 \qquad (1)$$

where μ_r is the relative magnetic permeability, ε_r the relative electrical permittivity and σ the electrical conductivity of the material ($S \cdot m^{-1}$); ε_0 is the electrical permittivity of the vacuum ($F \cdot m^{-1}$), k_0 the wave number in free space (m^{-1}), ω the wave angular frequency (s^{-1}) and $\bar{E}$ the electric field ($V \cdot m^{-1}$). The (1) has been computed by the Electromagnetic wave (EMW) feature with the following main boundary conditions [2]:

- Impedance boundary condition: The surfaces, shared between vacuum and the supporting solid material, are modeled in order to consider the losses due to the partial penetration of the electric field in the lossy material which constitutes such walls. This condition allows to exclude a further domain to the EMW calculation, avoiding the meshing and saving computational cost. The specified thickness of the wall boundaries is fixed to 80μm.
- Rectangular port: In order to allow EM energy enters or exits the waveguide, a rectangular port has been used to modeling the Waveguide port. This port is set to launch and absorb the TE_{10} mode of a rectangular waveguide. The average power input is 1 W. All the cold parameters of the cavity and the total power dissipation have been calculated in this step and stored in memory.

In order to evaluate the coupling between the cavity and the waveguide was useful to create a Smith chart on COMSOL. Since it is not present among the default plot menu, the Nyquist plot has been used with particular settings. Points of the Smith chart have been represented in function of the frequencies which compose the sweep for the analysis as the argument of exponential functions with different radii and centers. The Smith chart over the Nyquist plot is reported in figure 3, where the scattering parameter is superposed. The resonance tends to the critical coupling, as can be noted from the radius of the resonance circle which approaches to the unitary circle.

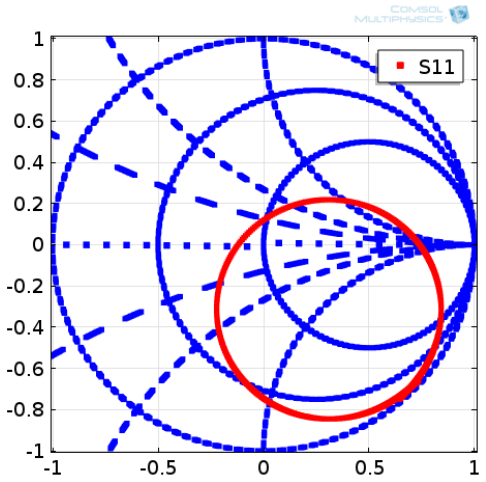

Figure.3. Smith Chart represented over the Nyquist plot. The Resonance circle is superposed to evaluate the coupling.

The electron source employed in this study is a carbon nanotube (CNT) emitter array that has dimensions obtainable with existing micromachining and photolithography processes, consistent with klystron operation at frequencies above 100 GHz. The e-Gun has been designed by following the theory of electron beam design reported in [11]. The beam dimensions are consistent with vacuum devices already studied in millimeter and sub-millimeter frequency range

[6]. The e-Gun is designed to produce a 16 mA beam of 10 keV electrons at the Buncher interface. This CNT device presents a cathode temperature of 35°C when operates at room temperature.

2.2 Heat Transfer and Fluid Flow

This computation step has been employed to couple TD and FD analysis [12]. These studies have been solved by adopting a fully coupled stationary calculation in order to evaluate the temperature distribution at the steady state, when the cathode temperature and cavity dissipations are fixed at operative values and the structure is subjected to an air flow of 2 ms^{-1} velocity oriented towards the lateral surface where is not present the input flange. In this condition the thermal equilibrium is reached since transient events are terminated.

Heat Transfer (HT) module of COMSOL has been computed by solving the Heat Equation in the steady state (2) [7].

$$-\nabla \cdot (k\nabla T) = Q \tag{2}$$

where k is the thermal conductivity ($W \cdot m^{-1} \cdot K^{-1}$) of the material and Q is the heat power density (Wm^{-3}). The power dissipation calculated in the previous Electromagnetic analysis has been prescribed on the Buncher walls as surface density power source, introducing another equation similar to (2) where the ∇ operator is replaced by a normal unitary vector and k has the negative sign ahead and the heat power density is given by the total electromagnetic losses.

The HT module has been set up with the following main boundary conditions:

- Heat transfer in Fluids: The non ideal vacuum and the air atmospheres inside the gun and Buncher volume are modeled only to describe the heat transfer and excluded from moment computations.
- Temperature: The temperature of the wall where the air flux enter inside the volume used to calculate the air flow (the air box) is set to the external temperature, fixed to T_{ext} = 25°C, consistently with a typical environment temperature condition. Another boundary condition is prescribed to the cathode surface, since it operates at 35°C.
- Heat source: The interior volume of the Buncher is a volume heat source defined through the total power dissipation density previously computed by a preliminary EM analysis computed as a first step.

The air motion is modeled with a single phase laminar flow and computed by solving the system of (3) and (4) in a stationary analysis [12] inserting the Laminar Flow (LF) feature of COMSOL.

$$\rho(u \cdot \nabla)u = \nabla \cdot \left[-pI + \mu\left(\nabla u + (\nabla u)^T\right) - \frac{2}{3}\mu(\nabla \cdot u)I \right] + F \tag{3}$$

$$\nabla \cdot (\rho u) = 0 \tag{4}$$

where p is the pressure, u is the velocity field ($m \cdot s^{-1}$), the material density ($kg \cdot m^{-3}$), μ the dynamic viscosity (Pa·s) of the material (the air) and F is the volume force ($N \cdot m^{-3}$). The symbol I stand for the identity matrix and T for the transposing operation. The LF computation has been performed including the following main boundary conditions:

- Inflow: The shortest side of the volume where the device is immerged has a boundary condition which imposes the input of the cooling airflow.
- Outflow: The opposite shortest side of the volume mentioned above has a boundary condition imposing the output of the cooling air flux.
- Symmetry: The widest side of the air box volume, where the device is immerged, has a boundary condition stating the symmetry with the corresponding opposite face. This allows reducing computational cost and it is allowed because the flux lines of the fluid flow are disposed in the same manner, internally to the virtual air box.

2.3 Solid Mechanics Analysis

The SM module received the output temperature from the previous computation and calculated the thermal displacements. Surfaces are in a stationary thermal regime, cooled by the external environment condition. The analysis has solved the stress steady state equation (5) fully coupled with the computation of the (2), (3) and

(4) by computing the thermal expansion of the materials [7].

$$-\nabla \cdot \sigma = \overline{F}_V \quad (5)$$

where σ is the stress (Nm^{-2}) and $\overline{F}_V$ is the force per unit volume (Nm^{-3}). The main boundary condition of this step is the fixed constraints: The external walls are free to move, except for the face where the cathode is mounted. This is modeled as fixed constraint because the device is supported from this face by the cathode assembly. The solid model is isotropic with quasi-static structural transient formulation.

2.4 Moving Mesh

After the HT, LF and SM analysis, the MM dedicated interface has been employed to produce deformed meshes in function of the displacements. Deformed meshes are used for the computation of the electromagnetic behavior. In the MM interface, the following features have been used [4]:

- Prescribed deformation: The structure of the gun and Buncher represent the volume subjected to deformation. The displacement vectors (u, v, w) computed by the SM module are employed to specify this volumetric deformation. Its prescribed mesh displacement is set to $d_x= u$, $d_y=v$, $d_z=w$.
- Free deformation: The non ideal vacuum and air volumes (which are not subjected to any structural elastic formulation by the SM analysis) are free to move. Initial deformation is set to $dx_0=0$, $dy_0=0$ and $dz_0=0$.
- Prescribed Mesh Displacement: This condition specifies that the surface boundaries shared between the volumes subjected to deformation and the ones free to move need to be deformed by the SM computation. This allows the free volume to follow the deformation of the volumes deformed by the SM step, though is attached to the free deformation air and non ideal vacuum boundaries. Such surfaces are subjected to deformation. This superficial displacement has been specified by setting the prescribed mesh displacement to $d_x= u$, $d_y=v$, $d_z=w$.

After this study, new mesh configuration has been produced. In the solution related to the MM study, it has been asked to the calculator to remesh deformed configuration. A "deformed configuration" sub-node appeared in the "Mesh" node on the model three. In such sub-node, has been asked to "build all". New meshes have been produced.

3. Thermomechanical Features

The airflow performs the device cooling as shown in fig 4, where the external maximum temperature approaches to 34.9°C. As shown in figure 5, the maximum temperature reached by the system is 35°C. In order to underline the deformation, stress and displacement are been plotted with a magnified scale. In the following figures, black outlines represent the original conformation, and the stained volume represents the deformed structure. As cold condition, the case of the sole EM computation is intended without Multiphysics computation. As thermomechanical operative condition, the concurrent action of both cathode heating and the cooling airflow at the same time is intended.

The global temperature distribution has induced a maximum stress of about 27.5 MNm^{-2} (figure6) located at the interfaces between the warmest face which is fixed to the rigid support. The internal shape, more free to deform, is less stressed than this interface. The maximum total displacement is located on the coolest face and is about 362 nm (figure 7). This is due to the low thermal expansion of silicon and to the fact that this face is at 25°C, only 5°C more than the reference temperature (20°C).

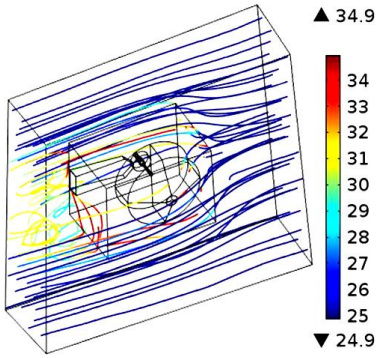

Figure 4. Airflow path with temperature distribution (°C).

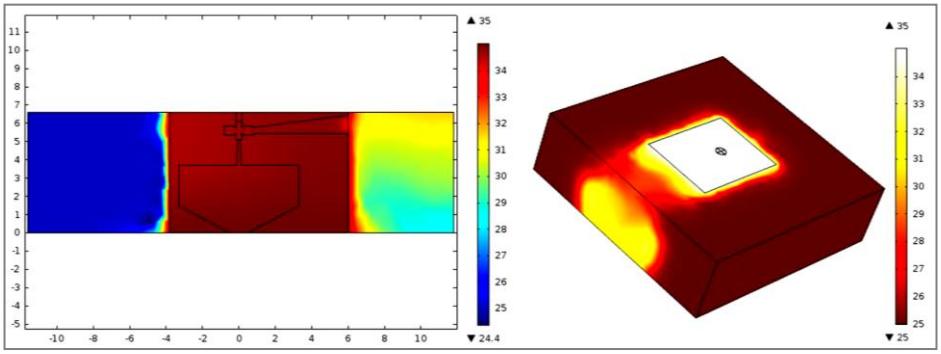
Figure 5. Temperature (°C): Cross sectional (left) and external 3D (right) views

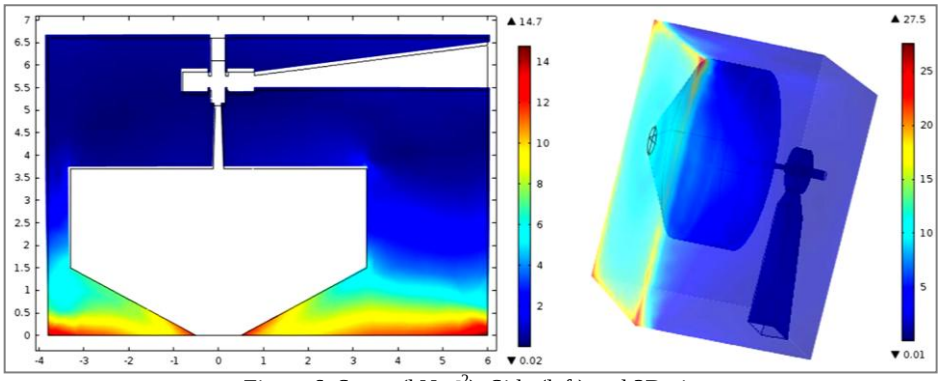
Figure 6. Stress (kNm^{-2}): Side (left) and 3D views

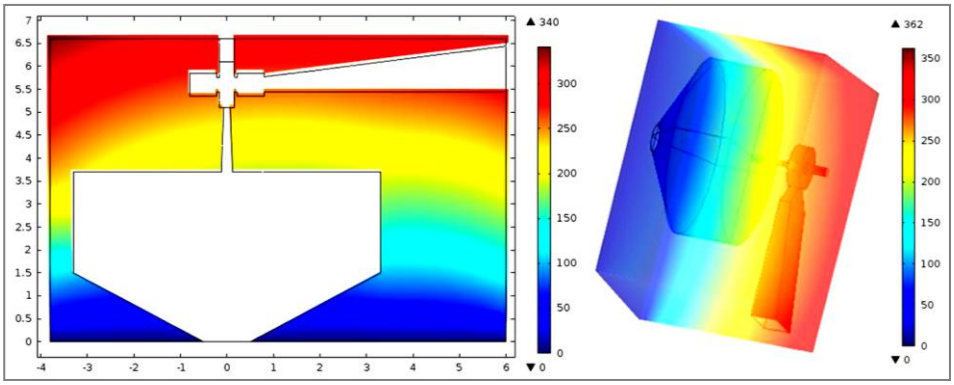
Figure 7. Displacement (nm): Side at centre (left) and 3D views.

4. Electromagnetic Features

The EMW analysis has given the following results. In figure 8 we can observe the streamline distribution of the electrodynamic fields for the bunching along the central plane. In cold and in thermo mechanical operating conditions respectively E_{ACmax} = 2.39 and E_{ACmax} = 2.99 MVm^{-1} are reached. The scattering parameters in cold and in TM operating conditions have been documented and reported in figure 9.

In this analysis has been considered also the case of thermal insulation of the device while it experiences the cathode heating. In this situation the system reach a thermal steady state at the cathode temperature of 35°C causing a considerable frequency lowering. This effect may happen if the system were enclosed in an insulated box, a situation preferably to be avoided. As shown in the red curve of figure 9, the resonance frequency of the Buncher from the cold condition (where it has the value of f_1=131.68 GHz) decreases to f_2 = 131.17 if only the thermal heating is present without cooling air flux. In this condition a difference of 510 MHz can be noted between the two frequencies. While the cooling air flux is operating, the controlled temperature at the Buncher lateral surfaces, it contains shape alteration. Anyhow, the base surface, where the beam output hole is located, tends to expanse straightly, since is less refrigerated, due to the positioning of the air flux streamlines which are crossed to longitudinal axis of the Buncher. This effect allows for a frequency increase dilating the gap, as shown in the purple curve of figure 9. In this condition, the resonance frequency moves to f_3=131.87. The axial dilation decreases the ratio between the surface and volume, decreasing the quality factor until decreasing the insertion loss to 18.7 to 18.4dB. This is a very small disadvantage if is compared to the advantage obtained over the frequency shift, which is decreased to 190 MHz, as discussed in the following text while treating the bunching field amplitude variation. This effect is dependent of the external shape which cannot modify the field in cold conditions but is determinant in operative conditions. It's evident as an opportune exterior shape can re-increase the performance of the device while it undergoes the operative influencing factors.

The longitudinal distribution of the electrodynamics bunching fields in cold and in thermo mechanical operating conditions is reported in figure 10. In this analysis, another effect has been highlighted: If the resonance frequency changes, is opportune to change the frequency of the load (typically a resonant device, such as a particle accelerator) connected to the Klystron in order to transfer the maximum power also in operative conditions. If the load operates at f_1 while the Klystron is operating to f_2 or f_3 due to the TM alterations, to the load a poor power can be transferred, since the bunching field at the cold frequency is reduced to less than an half (see purple curve in figure 10). If the load is online tuned to follow the operative frequency of the Klystron, the transferred power keep on be the same even if the frequency is shifted.

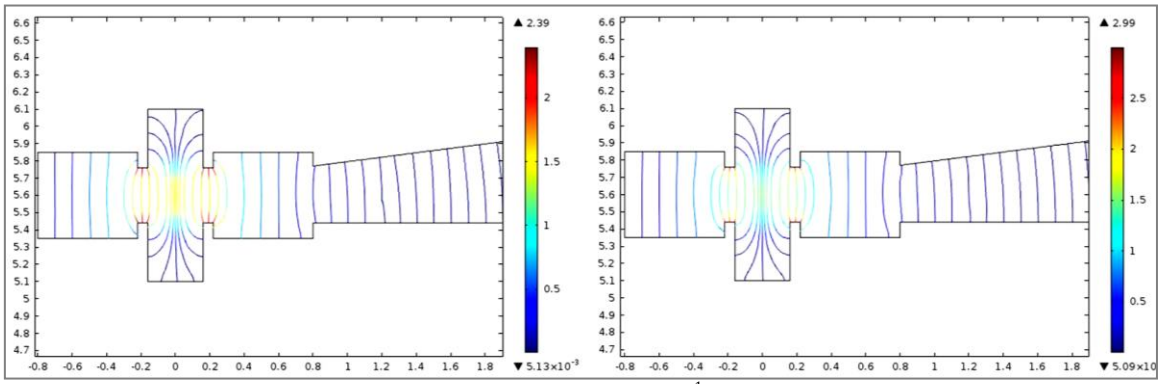

Figure 8. Streamline distribution of the electrodynamic fields MVm^{-1}: Cold and (left) working conditions (right).

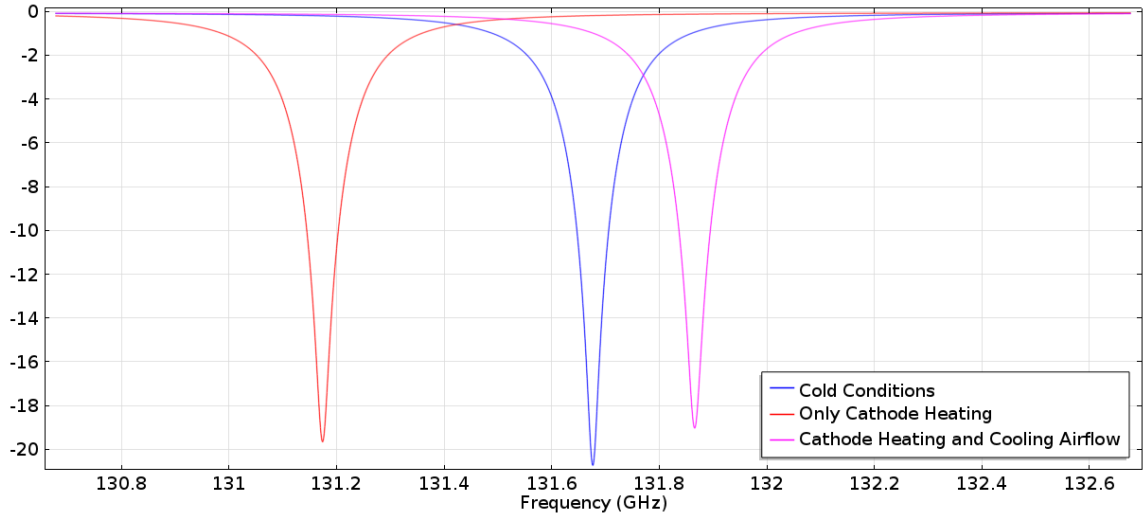

Figure 9. Scattering refection parameter S_{11} in dB: Cold and working conditions considering cooling airflow.

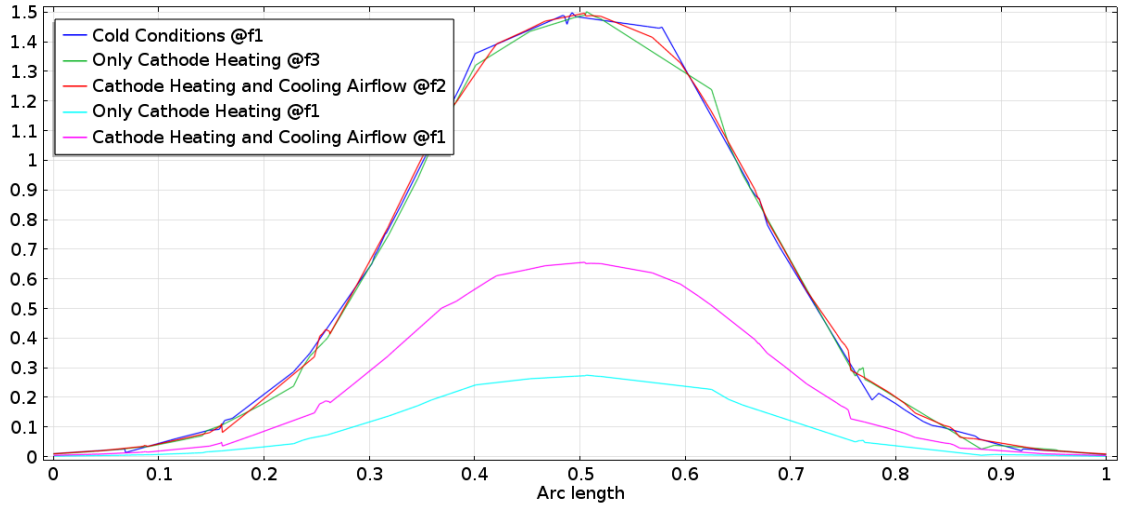

Figure 10. Axial electrodynamic field distribution (MVm^{-1}): Cold and working conditions, considering frequency shift.

5. Conclusions

The Multiphysics design of a 130 GHz klystron Buncher is described in this paper. Since heating effects and power dissipations modifies the electromagnetic behavior of the device an air flow has been used to control the temperature. In order to reduce thermal expansion, a Carbon nanotube cold cathode is employed operating at 35°C of temperature. The Thermo-mechanical modification of the Buncher due to the cathode heating and RF power dissipations affects the bunching electric field has been considered.

A multiphysics design on COMSOL Multiphysics have allowed for the estimation of the thermomechanically affected operation. A Thermo mechanical analysis has been performed by coupling Heat Transfer, Solid Mechanics and Laminar Flow modules. Temperatures and deformations have been determined, when the heat produced internally has been diffused to the whole system. Thermo-mechanical displacements have been computed and the Moving Mesh (MM) dedicated interface has been used to obtain the deformed geometry, where electromagnetic analysis is performed. Scattering parameters at the input port and axial electric field of the Buncher cavity have been calculated. The requirements for the air flow have been estimated.

This study shows the advantage of using cold cathode and cooling airflow, in order to reduce undesired thermal effects.

Several strategies have been adopted to obtain a simple but reliable model. The proposed approach has allowed to select the appropriate materials and geometries.

9. References

1. D. Passi, A. Leggieri, F. Di Paolo, M. Bartocci, A. Tafuto, A. Manna, "High Efficiency Ka-Band Spatial Combiner", *Advanced Electromagnetics*, Vol. 3, No. 2, page 10-15 (2014).

2. P.H. Siegel, A. Fung, H. Manohara, J. Xu, B. Chang, "Nanoklystron: A Monolithic Tube Approach to THz Power Generation". *Proc. of the Twelfth International Symposium on Space Terahertz Technology*, February 14-16, Shelter Island, San Diego, CA, USA, (2001).

3. M. C. Lin, D. N. Smithe, P. H. Stoltz, H. Song, and T. Kalkur, "A Microfabricated Klystron Amplifier for THz Waves", *Proc. of IVNC 2009*, page 189-190 (2009).

4. M. Mineo and C. Paoloni, "Micro Reentrant Cavity for 100 GHz Klystron", *Proc. of IEEE Vacuum Electronics Conference (IVEC)*, Monterey, CA, 2012, page .65-66 (2012).

5. C. Paoloni, M. Mineo, H. Yin, L. Zhang, W. He, C.W. Robertson, K. Ronald, A.D.R. Phelps and A.W. Cross, "Scaled Design and Test of a Coupler for Micro-Reentrant Square-Cavities for Millimeter Wave Klystrons", *Proc. of IEEE Vacuum Electronics Conference (IVEC)*, Paris, 2013, page 1-2 (2013).

6. A. Leggieri , G. Ulisse, F. Di Paolo, F. Brunetti, A. Di Carlo, "Particle tracing simulation of a vacuum electron gun for THz application", *Proc. of IEEE Millimeter Waves and THz Technology*, Rome (2013).

7. A. Leggieri, D. Passi, F. Di Paolo, "Key-Holes Magnetron Design and Multiphysics Simulation", *Proc. of COMSOL Conference 2013*, Rotterdam, NL (2013).

8. R. G. Carter, "Calculation of the Properties of Reentrant Cylindrical Cavity Resonators", *IEEE Transactions on Microwave Theory and Techniques*, Vol.55, Issue 12, (2007).

11. J. R. Pierce, *Theory and Design of Electron Beams*, D. Van Nostrand Company, Canada, The Bell Telephone Laboratories Series (1949).

12. COMSOL, *Heat transfer Module User's Guide*, COMSOL AB, Stockholm, page 69-72,111-212 (2012).